A Histone Deacetylase Complex Mediates Biofilm Dispersal and Drug Resistance in *Candida albicans*

Clarissa J. Nobile,[a,b] Emily P. Fox,[a,c] Nairi Hartooni,[a] Kaitlin F. Mitchell,[d] Denes Hnisz,[e]* David R. Andes,[d] Karl Kuchler,[e] Alexander D. Johnson[a]

Department of Microbiology and Immunology, University of California, San Francisco, San Francisco, California, USA[a]; Department of Molecular and Cell Biology, School of Natural Sciences, University of California, Merced, Merced, California, USA[b]; Tetrad Program, Department of Biochemistry and Biophysics, University of California, San Francisco, San Francisco, California, USA[c]; Department of Medicine, University of Wisconsin, Madison, Wisconsin, USA[d]; Medical University Vienna, Max F. Perutz Laboratories, Vienna, Austria[e]

* Present address: Denes Hnisz, Whitehead Institute for Biomedical Research, Cambridge, Massachusetts, USA.

ABSTRACT **Biofilms are resilient, surface-associated communities of cells with specialized properties (e.g., resistance to drugs and mechanical forces) that are distinct from those of suspension (planktonic) cultures. Biofilm formation by the opportunistic human fungal pathogen *Candida albicans* is medically relevant because *C. albicans* infections are highly correlated with implanted medical devices, which provide efficient substrates for biofilm formation; moreover, biofilms are inherently resistant to antifungal drugs. Biofilms are also important for *C. albicans* to colonize diverse niches of the human host. Here, we describe four core members of a conserved histone deacetylase complex in *C. albicans* (Set3, Hos2, Snt1, and Sif2) and explore the effects of their mutation on biofilm formation. We find that these histone deacetylase complex members are needed for proper biofilm formation, including dispersal of cells from biofilms and multifactorial drug resistance. Our results underscore the importance of the physical properties of biofilms in contributing to drug resistance and dispersal and lay a foundation for new strategies to target biofilm dispersal as a potential antifungal intervention.**

IMPORTANCE **Through the formation of biofilms—surface-associated communities of cells—microorganisms can establish infections, become drug resistant, and evade the host immune system. Here we investigate how four core members of a conserved histone deacetylase complex mediate biofilm formation by *Candida albicans*, the major fungal pathogen of humans. We show that this histone deacetylase complex is required for biofilm dispersal, a process through which cells leave the biofilm to establish new infections. We also show that the deacetylase complex mediates biofilm drug resistance. This work provides new insight into how the physical properties of biofilms affect dispersal and drug resistance and suggests new potential antifungal strategies that could be effective against biofilms.**

Received 25 April 2014 **Accepted** 19 May 2014 **Published** 10 June 2014

Citation Nobile CJ, Fox EP, Hartooni N, Mitchell KF, Hnisz D, Andes DR, Kuchler K, Johnson AD. 2014. A histone deacetylase complex mediates biofilm dispersal and drug resistance in *Candida albicans*. mBio 5(3):e01201-14. doi:10.1128/mBio.01201-14.

Editor John W. Taylor, University of California, Berkeley

Address correspondence to Clarissa J. Nobile, cnobile@ucmerced.edu.

This article is a direct contribution from a member of the American Academy of Microbiology.

Biofilms are organized, surface-associated communities of microorganisms with important medical impact. Biofilms are notorious for forming on various implanted medical devices, including catheters, pacemakers, heart valves, dentures, and prosthetic joints, which provide a surface and sanctuary for biofilm growth (1, 2). As a result, the human health consequences of device-associated infections can be severe and often life-threatening (3). Biofilms of *Candida albicans*, the major fungal pathogen of humans, cause bloodstream and device-associated infections with high mortality rates approaching 40% (2, 4–6). *C. albicans* biofilms are resistant to standard antifungal drugs; not only do biofilms provide physical protection from drugs, cells in biofilms become intrinsically resistant to antimicrobial compounds because of their altered metabolic states and their constitutive upregulation of drug efflux pumps (7–10). These and other characteristics of *C. albicans* biofilms—which are not observed in planktonic/suspension cultures—make biofilm formation a significant virulence factor for this opportunistic pathogen.

C. albicans biofilm development *in vitro* occurs in four basic stages (5, 11–15), (i) attachment and colonization of round budding yeast cells to a surface, (ii) growth and proliferation of yeast cells to produce a basal layer of anchoring cells, (iii) growth of ellipsoid pseudohyphae and extensive elongated cylindrical hyphae along with the production of the extracellular matrix, and (iv) dispersal of yeast cells from the biofilm to seed new sites. Of all of the stages of biofilm development, the dispersal step is the least understood in molecular terms.

Using genome-wide approaches, the transcriptional network that orchestrates the development of *C. albicans* biofilms was recently described (16). It consists of six "master" transcriptional regulators (sequence-specific DNA-binding proteins) that control each other's expression and the expression of over 1,000 down-

stream target genes (16, 17). The six master regulators (Bcr1, Tec1, Efg1, Ndt80, Rob1, and Brg1) are arranged together in a tightly interwoven transcriptional network. Among the 52 transcriptional regulators that are direct targets of at least one of the master biofilm regulators of the network, the transcriptional regulators Sfu1, Crz2, and Nrg1 are the only direct targets of all six of the master biofilm regulators (16, 17). Not surprisingly, Sfu1, Crz2, and Nrg1 have been implicated in various aspects of biofilm formation; Sfu1 represses iron uptake genes and enhances commensalism in the gastrointestinal tract (18) and thus may play a role in biofilm formation on mucosal surfaces in the gut; Crz2 is required for the first step of biofilm formation, adherence of yeast cells to a surface (19); and Nrg1 is a key regulator of biofilm dispersal (20), where induced expression of *NRG1* during biofilm formation increases the dispersal of yeast cells over time. Overall, these nine transcriptional regulators (six master regulators and three "downstream" regulators that are direct targets of the biofilm master regulators) are involved in various key aspects of *C. albicans* biofilm formation.

Recently, it has been demonstrated that chromatin and chromatin-modifying enzymes are important for mediating the expression of morphogenesis-related genes in *C. albicans* (21, 22). For example, the Hda1 histone deacetylase and the NuA4 histone acetyltransferase mediate histone deacetylation and acetylation, respectively, at the promoters of hypha-specific genes (22). In addition, mutations in genes encoding some chromatin modifiers, such as the Set1 histone methyltransferase, the Rtt109 histone acetyltransferase, and the Set3 histone deacetylase, have abnormal morphogenesis-related phenotypes (23–26). Using a combination of genome-wide chromatin immunoprecipitation, followed by sequencing, and RNA sequencing (RNA-seq), Hnisz et al., recently identified the regulatory target genes of the *C. albicans* Set3 complex, an NAD-dependent histone deacetylation complex, and found that the complex modulates the transcription kinetics of several morphogenesis-related transcriptional regulators (23). Specifically, they demonstrated that the Set3 complex binds directly to the coding regions of five of the six master biofilm regulators, *BRG1*, *TEC1*, *EFG1*, *NDT80*, and *ROB1*, as well as the "downstream" regulator *NRG1* (23). These results suggest that the Set3 complex may have an important role in *C. albicans* biofilm development.

With sequence conservation from fungi to humans, the Set3 complex was first identified as a repressor of sporulation in baker's yeast, *Saccharomyces cerevisiae* (27). In *S. cerevisiae*, the Set3 complex consists of seven distinct subunits; Hos2, Sif2, Snt1, and Set3 form the functional core complex (necessary for stability of the complex), while Hst1, Cpr1, and Hos4 act as peripheral subunits (27). In *C. albicans*, only the core complex has been studied and, as discussed above, was recently found to be involved in the modulation of morphogenesis-related processes (23, 24). Here, we test whether the core Set3 complex is needed during *C. albicans* biofilm formation and find that it is involved in the regulation of two specific and important aspects of biofilm formation, (i) dispersal of cells from a mature biofilm and (ii) antimicrobial drug resistance specifically within the context of a biofilm.

RESULTS

Set3 complex mutants form distinctive biofilms. We tested four constructed core Set3 complex homozygous deletion mutants of *C. albicans* (*hos2*Δ/Δ, *sif2*Δ/Δ, *snt1*Δ/Δ, and *set3*Δ/Δ) (24, 28, 29) for the ability to form biofilms on the surface of a polystyrene plate under a standard set of *in vitro* biofilm-inducing conditions (14, 30). The phenotypes of the biofilms produced were assessed by visual examination *in vitro*, by confocal scanning laser microscopy (CSLM) inspection *in vitro*, by biofilm dry-weight biomass measurements *in vitro*, and by scanning electron microscopy (SEM) inspection *in vivo* in a rat catheter animal model. Upon visual inspection of the biofilms formed by the four Set3 complex mutants *in vitro*, it was apparent that these biofilms differed from those of the parent strain, displaying a distinctive "rubbery" phenotype. To probe this novel phenotype further, we developed an *in vitro* perturbation assay in a six-well plate, where a plastic pipette was used to agitate the biofilms and lift the intact biofilms above the plate (Fig. 1A to E). Agitation of the biofilm of the wild-type reference strain in this manner caused the biofilm to break apart in the well (Fig. 1A). Unexpectedly, the biofilms of all four Set3 complex mutants were impervious to this perturbation and remained completely physically intact (Fig. 1B to E). To determine whether biofilms formed by the Set3 complex mutant strains have obvious differences in cell morphology from the wild-type reference strain, we characterized the biofilms formed by the four Set3 complex mutant strains by CSLM *in vitro* by using silicone squares as substrates. By CSLM, the wild-type reference strain and all four Set3 complex mutant strains formed mature biofilms with typical architecture and thickness (5, 13, 14, 16) after 24 h of development (Fig. 1F to J [top views] and K to O [side views]). CSLM of older 48-h biofilms of the Set3 complex mutant strains and the wild-type strain was also performed, and no obvious morphological differences were observed (see Fig. S1 in the supplemental material). To assess whether the biofilms formed by the Set3 complex mutant strains have biomass differences from the wild-type reference strain, we measured the dry-weight biomasses of the biofilms formed by the four Set3 complex mutant strains and found small but significant and reproducible differences (Fig. 2). All four Set3 complex mutants had enhanced biofilm biomasses ($P = 0.01$ for *hos2*Δ/Δ, $P = 0.02$ for *sif2*Δ/Δ, $P = 0.01$ for *snt1*Δ/Δ, and $P = 0.04$ for *set3*Δ/Δ), compared to the wild-type reference strain. As a complementary assay, we also performed crystal violet staining of the biofilms of the strains and found statistically significantly greater dye uptake by all four Set3 complex mutants than by the wild type (Fig. S2), consistent with the dry-weight assays.

Biofilm formation *in vivo* comprises several additional elements that are absent from our *in vitro* model, including liquid flow rates and the presence of host factors, such as components of the host immune response (31). For this reason and because biofilm-based catheter infections are a major clinical issue (2), we characterized a subset of the Set3 complex mutants in an *in vivo* central venous catheter biofilm model (32). Because all four of the core Set3 complex mutants behaved similarly in our *in vitro* biofilm assays (and to use as few animals as possible), we chose to test two complex mutants (*hos2*Δ/Δ and *set3*Δ/Δ) *in vivo*. We inoculated the catheters with *C. albicans* cells intraluminally, allowed biofilm formation to proceed for 24 h, removed the catheters, and visualized the catheter luminal surfaces by SEM (Fig. 3). The wild-type reference strain and the *hos2*Δ/Δ and *set3*Δ/Δ mutant strains all formed thick, mature biofilms consisting of yeast and hyphal cells and extracellular matrix material on the rat catheter (Fig. 3A to C [high magnification] and D to F [low magnification]). Consistent with our *in vitro* findings, there were no apparent morpho-

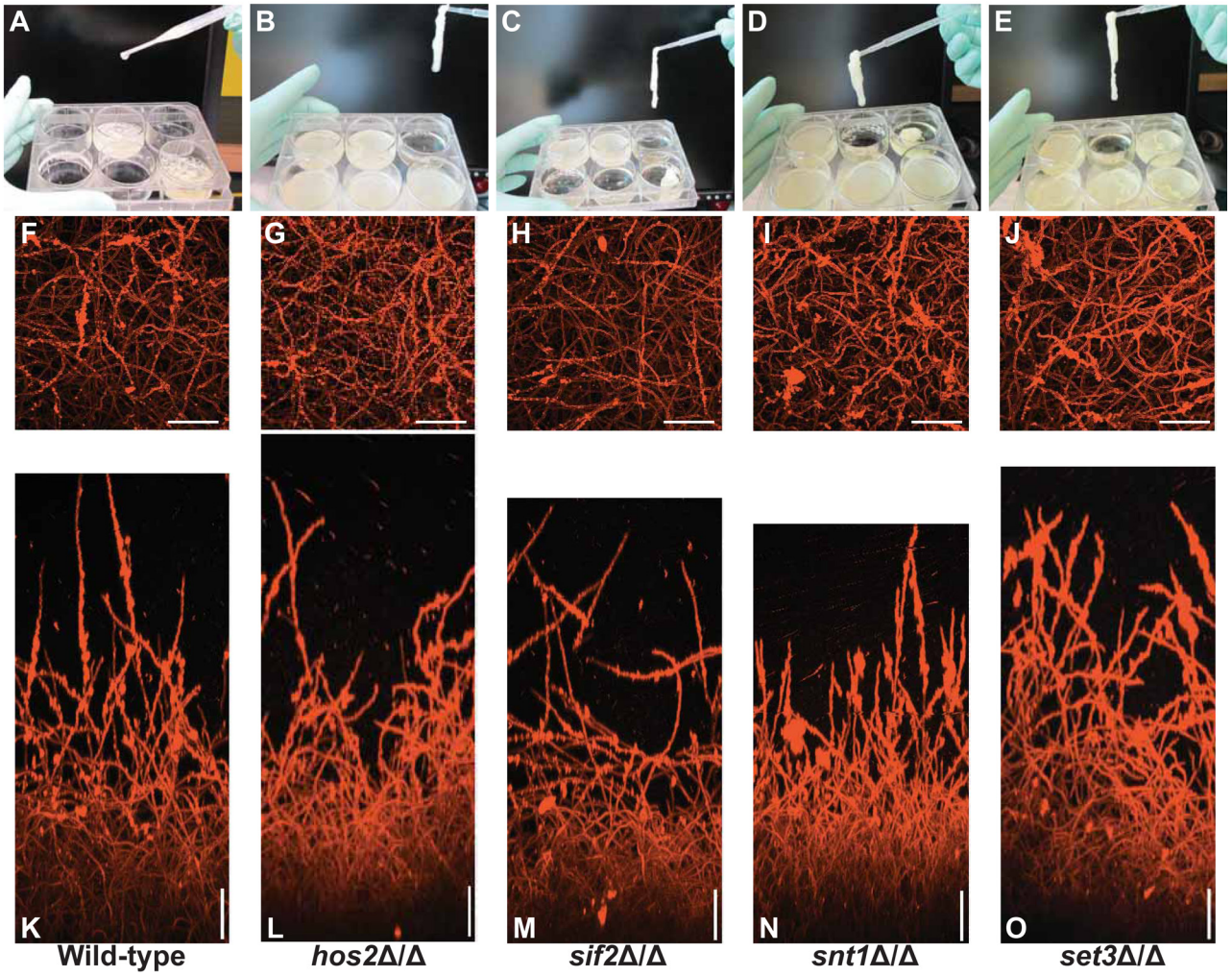

FIG 1 Phenotypic characterization of the biofilms formed by Set3 complex mutants. The top row shows the visual appearance of the biofilm perturbation assays for the wild type (A) and the *hos2*Δ/Δ (B), *sif2*Δ/Δ (C), *snt1*Δ/Δ (D), and *set3*Δ/Δ (E) mutants. the middle and bottom rows show top (F to J)- and side (K to O)-view CSLM images of the wild-type and Set3 complex mutant strains after 24 h of growth. Scale bars represent 50 μm.

logical differences between the biofilms formed by the strains *in vivo*. We did, however, observe that the constituents (yeast cells, hyphae, matrix, host cells, and host components) of the *in vivo* biofilms formed by the *hos2*Δ/Δ and *set3*Δ/Δ mutants were exceptionally sticky (they stuck both to each other and to the catheter lumen), consistent with the "rubbery" phenotype that we observed *in vitro*.

The Set3 complex modulates biofilm dispersal. On the basis of our observations that the biofilms formed by the four Set3 complex mutants were enhanced in biomass and distinctively resistant to physical perturbation, we hypothesized that the Set3 complex mutant biofilms may inappropriately retain cells within the biofilm. To test this hypothesis, we developed two types of biofilm dispersal assays (see Materials and Methods), (i) a standard-dispersal assay and (ii) a sustained-dispersal assay. For both assays, we used both wild-type and *nrg1*Δ/Δ mutant strains as references for biofilm dispersal; previous work has shown that ectopically induced expression of *NRG1* during biofilm formation increases the dispersal of yeast cells from a biofilm in a flow model (20). We used an *nrg1*Δ/Δ mutant strain, as we predicted this strain should be defective in dispersal in our assays. For the standard biofilm dispersal assay, biofilms were prepared (including a washing step after adherence) by following a standard protocol (see Materials and Methods) and cell dispersal was assessed after 24 h by carefully removing all of the medium from each well without disturbing the biofilm adhering to the bottom of the well. The optical density at 600 nm (OD_{600}) of the medium removed was measured, fresh medium was then added to the well, and biofilm formation was allowed to proceed. Two additional OD_{600} readings were taken at 48 and 60 h following this procedure. For the sustained biofilm dispersal assay, biofilms were prepared by following a standard protocol and cell dispersal was assessed after 24, 48, and 60 h by carefully removing all of the medium from each well without disturbing the biofilm adhering to the bottom of the well, and the OD_{600} of the medium removed at each time point was measured. The primary difference between the standard and sustained-dispersal assays was that in the sustained-dispersal assay, OD_{600} readings were taken over time as the biofilms were grown in the original medium, without the addition of fresh medium. As a planktonic growth control for later time points in the

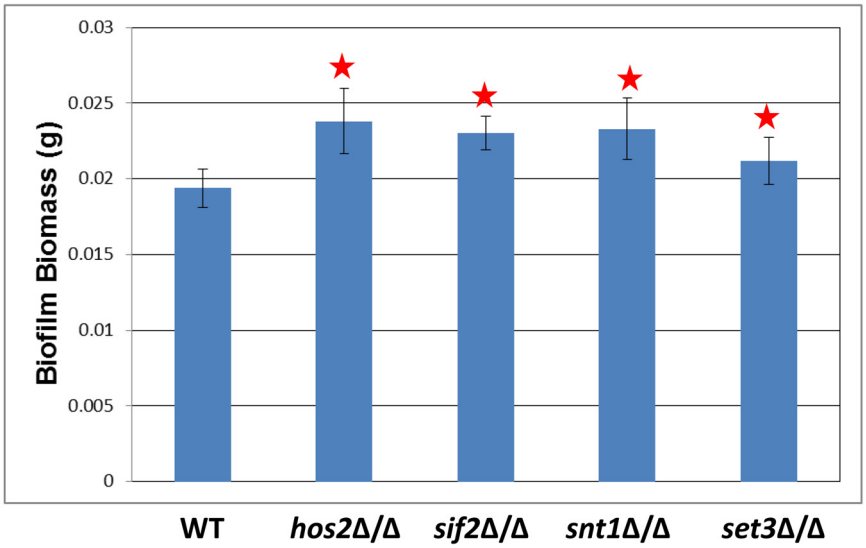

FIG 2 Biofilm biomass of Set3 complex mutants. The average total biomass ± the standard deviation for each Set3 complex mutant strain grown under standard biofilm conditions was calculated from five independent samples of each strain. Statistical significance (*P* values) was calculated with Student's one-tailed paired *t* test and is represented by the red star indicating the four Set3 complex mutant strains (*hos2*Δ/Δ, *sif2*Δ/Δ, *snt1*Δ/Δ, and *set3*Δ/Δ) with biomasses significantly differing ($P < 0.05$) from that of the wild-type (WT) reference strain.

sustained biofilm dispersal assay, cells suspended in the medium removed from above the biofilm samples were grown planktonically in the same biofilm spent medium over the same time points measured in the sustained biofilm dispersal assay and OD_{600} readings were taken. No planktonic growth was observed in the biofilm spent medium over time (data not shown), indicating that the sustained biofilm dispersal assay measures cells dispersed after growth of the biofilm rather than planktonic growth of initially dispersed cells. We note that quantitative CFU counts of dispersed cells in the biofilm spent medium from the wild type and Set3 complex mutants showed similar levels of cell viability in the mutant and wild-type strains (data not shown). First, we verified that the *nrg1*Δ/Δ mutant strain was significantly defective in dispersal compared to the reference strain at every time point measured in both the standard and sustained biofilm dispersal assays ($P < 0.002$, Fig. 4). In the standard-dispersal assay, where fresh medium was added after OD_{600} determination at each time point, the wild-type reference strain dispersed a moderate number of cells over time (Fig. 4A to C). In the sustained-dispersal assay, the wild-type reference strain dispersed an increasing number of cells over time (Fig. 4D to F) and the number of dispersed cells was highest at the latest time point taken (Fig. 4F). When we tested the Set3 complex mutants in both assays, we found that all four of them were significantly defective (compared to the reference strain) in both biofilm dispersal assays at every time point examined ($P < 0.005$, Fig. 4).

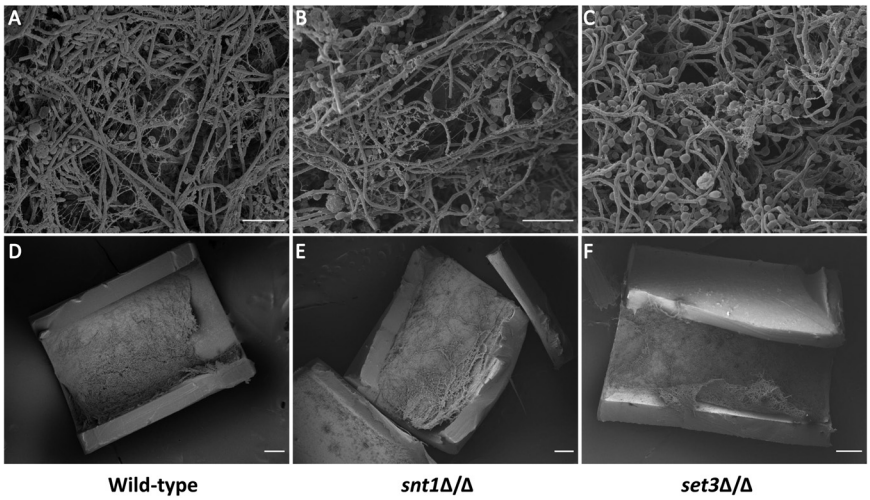

FIG 3 Biofilm formation of Set3 complex mutants in a rat catheter *in vivo* model. Wild-type reference strain SN425 (A and D) and Set3 complex mutant strains CJN2775 (*snt1*Δ/Δ) and CJN2770 (*set3*Δ/Δ) (B, C, E, and F) were inoculated into rat intravenous catheters, and the resulting biofilms were visualized after 24 h of growth by SEM. These SEM images show catheter luminal surfaces at high (A to C) and low (D to F) magnifications. Scale bars represent 20 μm in high-magnification images and 200 μm in low-magnification images.

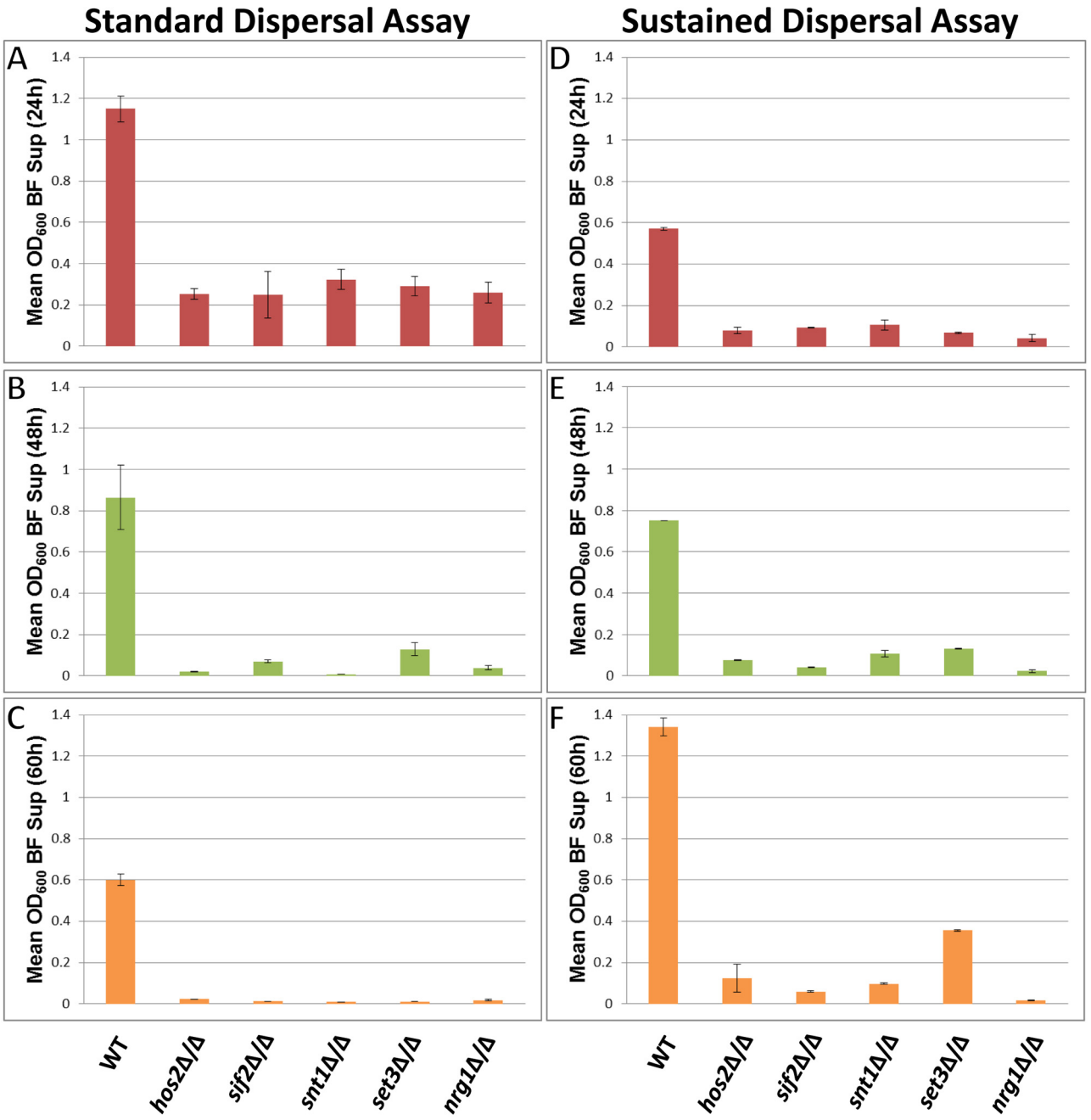

FIG 4 Biofilm dispersal assays of Set3 complex mutants. Standard-dispersal (A·to C) and sustained-dispersal (D to F) assays at three time points (24, 48, and 60 h) are shown. Five replicate wells were used for each strain.

The Set3 complex modulates biofilm drug resistance. To further explore the properties of the biofilms formed by the Set3 complex mutants, we assessed the drug resistance of the four core Set3 complex mutants under both planktonic and biofilm conditions. To assess drug susceptibility under planktonic conditions, we performed standard MIC assays (33) of the mutants and the wild-type reference strain with five highly effective fungicidal or fungistatic drugs (1,10-phenanthroline, 4-nitroquinoline *N*-oxide, caspofungin acetate, amphotericin B, and fluconazole) by using OD_{600} values as an output. (1,10-Phenanthroline and 4-nitroquinoline *N*-oxide were chosen on the basis of our experiences with their efficacy against biofilms; caspofungin acetate, amphotericin B, and fluconazole were chosen as representatives of the standard classes of antifungals used clinically.) All five drugs inhibited planktonic growth of the wild-type reference strain at concentrations consistent with previously published values. We note that only four of the five drugs inhibited biofilm formation; fluconazole had no observable effect at concentrations as high as 25 μg/ml, which is consistent with the published literature. The results of the standard planktonic MIC assay indicated that all of the Set3 complex mutants behaved similarly to the wild-type reference strain, with similar levels of killing or growth inhibition by

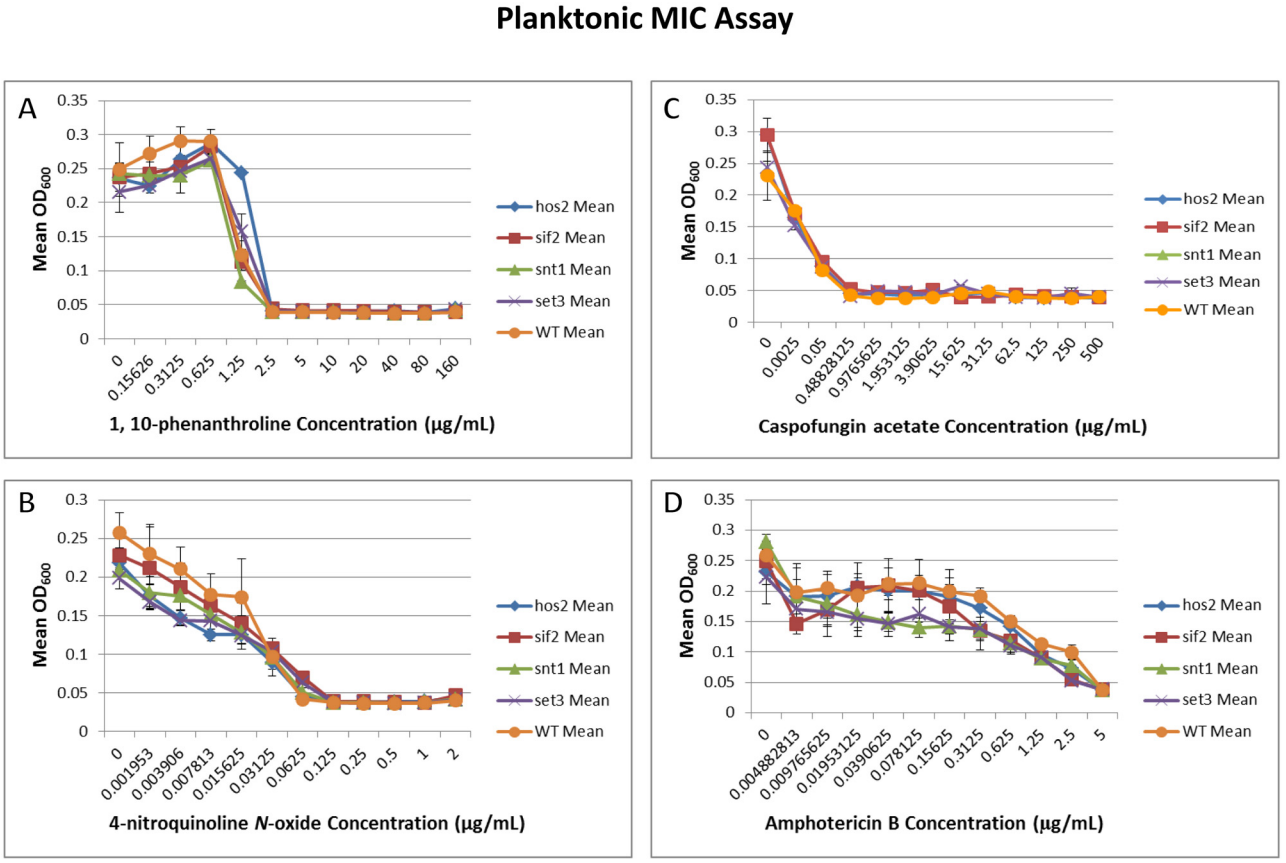

FIG 5 Planktonic drug MIC assays. For planktonic MIC assays, 1,10-phenanthroline was tested at concentrations of 160 μg/ml down to 0 μg/ml in 2-fold dilution steps (A), 4-nitroquinoline *N*-oxide was tested at concentrations of 2 μg/ml down to 0 μg/ml in 2-fold dilution steps (B), caspofungin acetate was tested at 100 μg/ml down to 0 μg/ml in various dilution steps (C), and amphotericin B was tested at 5 μg/ml down to 0 μg/ml in 2-fold dilution steps (D). MIC assays were performed in triplicate. Mean OD_{600} readings are reported with standard errors. BF Sup, biofilm supernatant; WT, wild type.

1,10-phenanthroline (Fig. 5A), 4-nitroquinoline *N*-oxide (Fig. 5B), caspofungin acetate (Fig. 5C), amphotericin B (Fig. 5D), and fluconazole (data not shown). To assess drug susceptibility under biofilm conditions, we performed a biofilm drug disruption assay of mature 24-h biofilms (see Materials and Methods), where these drugs were added for an additional 24 h of incubation after the biofilm was formed, the medium containing disrupted cells was removed, and the OD_{600} of the remaining biofilm on the bottom of the plate was read. These results showed that the biofilms of all Set3 complex mutants were significantly more resistant to 1,10-phenanthroline ($P < 0.05$, Fig. 6A), 4-nitroquinoline *N*-oxide ($P < 0.05$, Fig. 6B), caspofungin acetate ($P < 0.05$, Fig. 6C), and amphotericin B ($P < 0.05$, Fig. 6D) than the wild type was. To determine if the cells retained in the biofilms of the Set3 complex mutant and wild-type strains were viable, we performed quantitative CFU counting of the biofilms remaining in the wells after extensive mechanical disruption of the biofilms (see Materials and Methods). We found that the biofilms of the Set3 complex mutants contained a higher proportion of viable cells by comparing drug treatment relative to no treatment relative to the wild type (Fig. 7). An additional standard assay of biofilm cell viability, the 2,3-bis(2-methoxy-4-nitro-5-sulfophenyl)-2*H*-tetrazolium-5-carboxanilide (XTT) assay, was also performed. This test showed that the 4-nitroquinoline-*N*-oxide- and amphotericin B-treated biofilms of the Set3 complex mutants contained higher proportions of viable cells than the wild type biofilms did (see Fig. S3 in the supplemental material). Because of the high day-to-day variation of the Set3 complex mutants in the XTT assay, we believe that the quantitative biofilm CFU viability assay (Fig. 7) more accurately assesses the cell viability of these mutants.

We tested whether increased drug resistance of the Set3 complex mutants was due to the upregulation of the multidrug transporters of the ATP-binding cassette (ABC) superfamily. We did not detect significant changes (assessed by quantitative PCR) in the transcriptional levels of the major multidrug ABC transport efflux pumps (*CDR1*, *CDR2*, and *CDR3*) in planktonic cells (see Fig. S4A in the supplemental material) or biofilms (see Fig. S4B) of the Set3 complex mutants relative to the wild type.

The biofilm-specific resistance of the Set3 complex mutant strains was also not due to alterations in cell membrane integrity, as there were no detectable differences in lipid permeability in either planktonic cells or biofilms of the Set3 complex mutants relative to the wild type, as determined by a fluorescein diacetate (FDA) enzymatic uptake assay (34), which measures passive membrane diffusion by using a probe that is fluorescently activated upon hydrolysis by intracellular esterases (see Fig. S5 in the supplemental material). These observations suggest that the resistance of the Set3 complex mutant biofilms is likely the result of some other biofilm-specific physical attribute. One physical factor

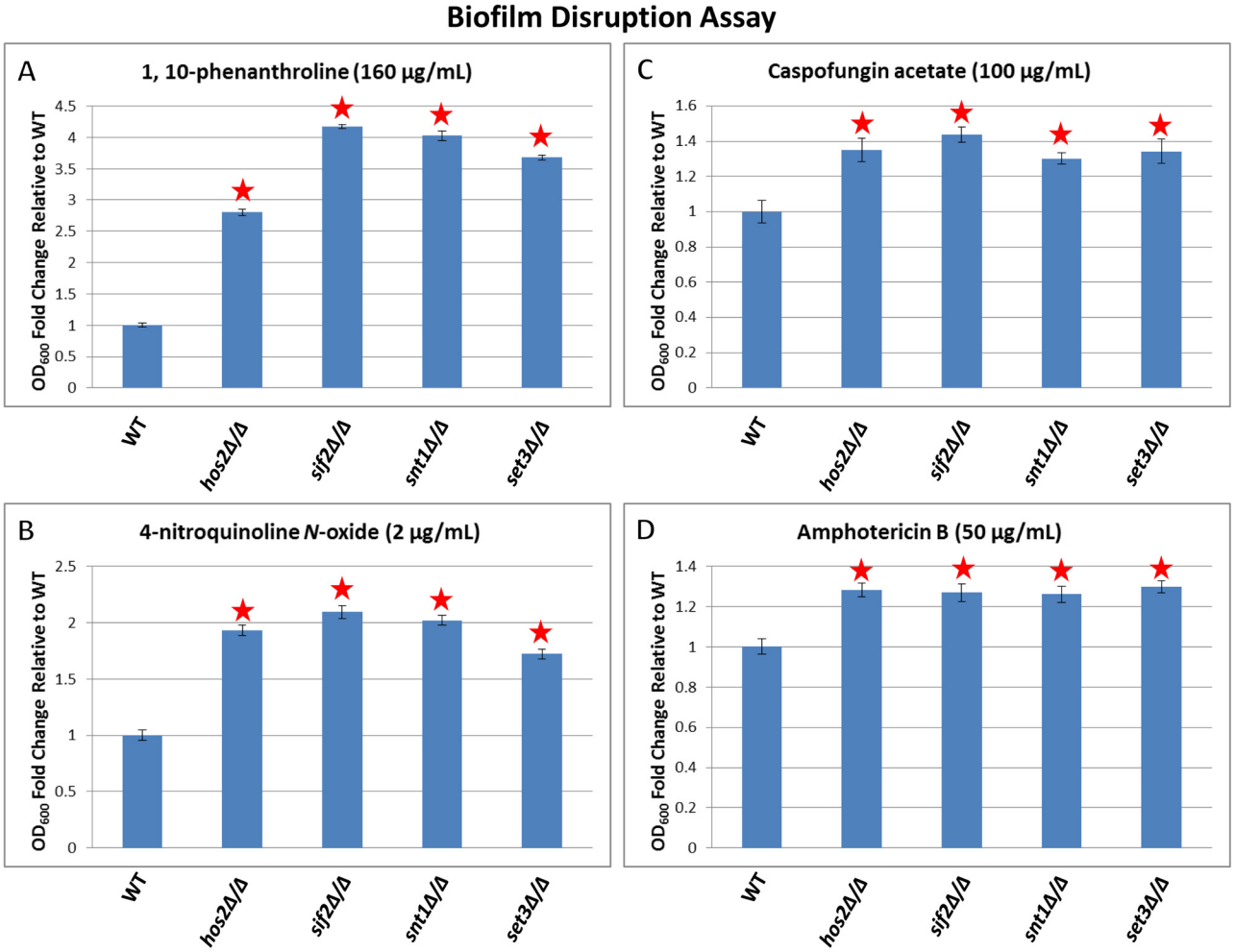

FIG 6 Drug biofilm disruption assays. In biofilm disruption assays, 1,10-phenanthroline was tested at a concentration of 160 μg/ml (A), 4-nitroquinoline *N*-oxide was tested at a concentration of 2 μg/ml (B), caspofungin acetate was tested at a concentration of 100 μg/ml (C), and amphotericin B was tested at a concentration of 50 μg/ml (D). Fold changes in the with/without drug treatment ratios of the OD_{600} values of mutants relative to the wild-type (WT) OD_{600} ratio are shown, and the wild-type OD_{600} ratio was set to 1.0. Five replicate wells were used for each condition. Statistical significance (*P* values) was calculated with Student's one-tailed paired *t* test and is represented by red stars indicating the four Set3 complex mutant strains (*hos2*Δ/Δ, *sif2*Δ/Δ, *snt1*Δ/Δ, and *set3*Δ/Δ) with OD_{600} values significantly differing ($P < 0.05$) from that of the wild-type reference strain.

known to contribute to drug resistance during biofilm formation is the extracellular matrix, specifically, the β-1,3-glucan component of the matrix (35). However, we found that biofilms formed by the Set3 complex mutants did not contain more β-1,3-glucan in the matrix of their biofilms (see Fig. S6 in the supplemental material), ruling out this hypothesis for increased drug resistance.

DISCUSSION

Our results highlight the importance of a conserved chromatin-modifying complex in the regulation of gene expression during biofilm formation. This complex binds directly to the coding regions of five out of the six biofilm "master" regulators (*BRG1*, *TEC1*, *EFG1*, *NDT80*, and *ROB1*), three of which (*BRG1*, *TEC1*, and *EFG1*) show altered transcription kinetics in *set3*Δ/Δ mutant cells (16, 23). Given these results, it is perhaps not surprising that the Set3 complex has a role in biofilm development. What is surprising, however, is the specificity of the defects produced by deleting any member of the complex. Moreover, these defects do not simply phenocopy those produced by the deletion of any one of the master biofilm transcriptional regulators, indicating a level of complexity in the genetic circuit hierarchy that was not previously recognized. In particular, deletion of any of the Set3 core subunits produces a previously undescribed phenotype consisting of enhanced cohesiveness, increased resistance to physical perturbation, decreased dispersal, and increased drug resistance.

The Set3 complex is known to modulate the transcription kinetics of *NRG1* (23), a transcriptional regulator of biofilm dispersal (20). It is possible that the Set3 complex acts, at least in part, by controlling levels of *NRG1*. This makes sense in light of the facts that Nrg1 is a transcriptional repressor of filamentation, that the Set3 complex mutants are hyperfilamentous (23), and that cells typically dispersed from *C. albicans* biofilms have been found to exist in the yeast form (15, 20). Thus, manipulations that increase filamentous cells and decrease yeast-form cells may reduce biofilm dispersal.

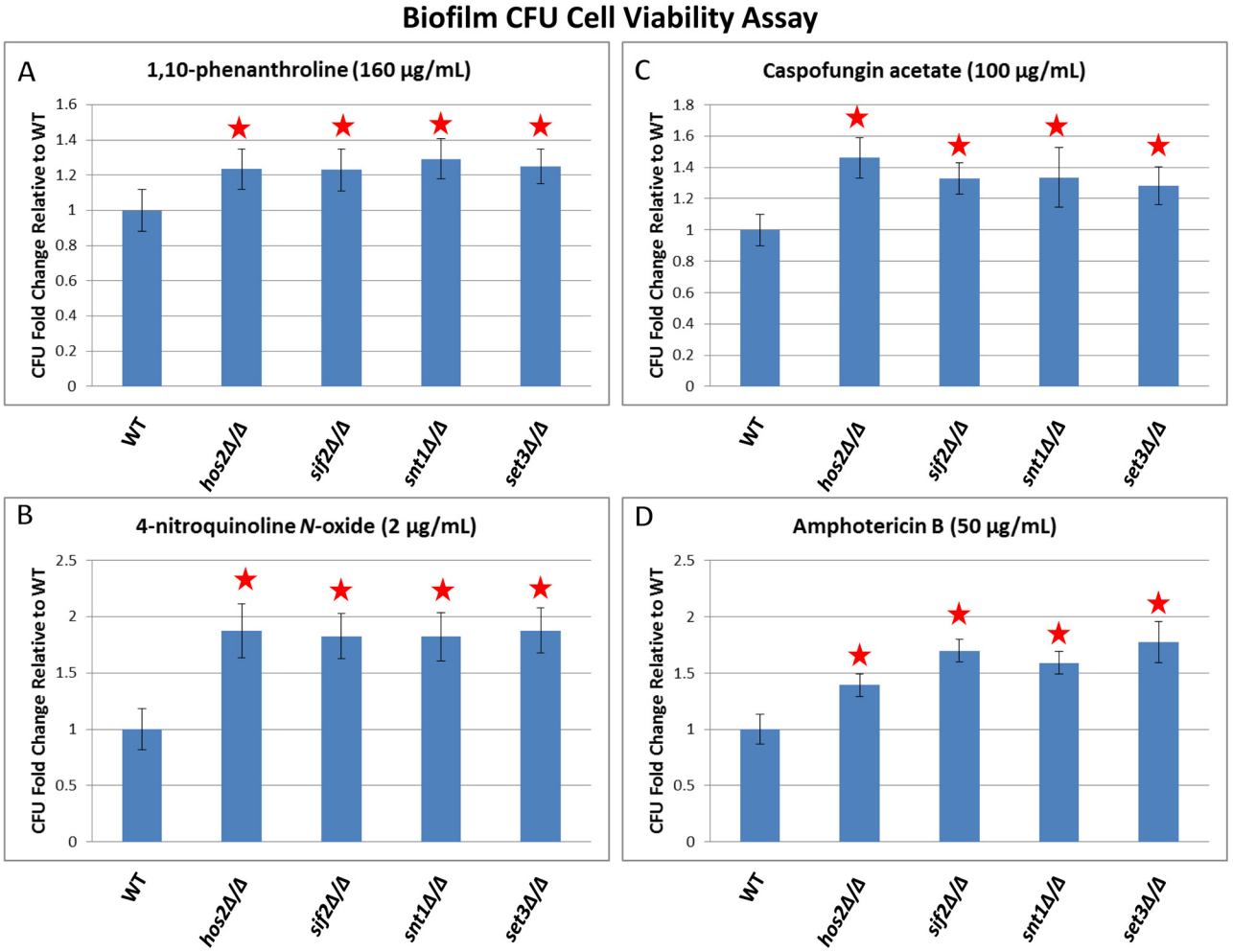

FIG 7 Biofilm cell viability CFU assays. The viable biofilm cell burden was determined after drug treatment by physical disruption of the biofilm remaining at the bottom of the well, followed by serial dilutions, plating, and CFU counting. The average of four dilutions from five wells is shown. Fold changes in the with/without drug treatment ratios of the CFU counts of mutants relative to the wild-type (WT) CFU count ratio are shown, and the wild-type CFU count ratio was set to 1.0. Statistical significance (*P* values) was calculated with Student's one-tailed paired *t* test and is represented by red stars indicating the four Set3 complex mutant strains (*hos2*Δ/Δ, *sif2*Δ/Δ, *snt1*Δ/Δ, and *set3*Δ/Δ) with CFU counts significantly differing ($P < 0.05$) from that of the wild-type reference strain.

Dispersal is the least understood and perhaps most complicated stage of the biofilm life cycle of both fungi and bacteria. In bacterial biofilms, dispersal is triggered by several signal transduction pathways, effector molecules, and environmental cues that often act in concert (36, 37). In terms of virulence, very few studies have directly assessed the role of biofilm dispersal in pathogenesis. There is, however, anecdotal evidence to suggest that the ability to disperse from bacterial biofilms is important for disease progression by allowing dispersed cells to colonize new niches within the host and suggesting a means through which a minor local infection could transition to a severe systemic infection. For example, the *smcR* mutant of the marine pathogen *Vibrio vulnificus*, which exhibits decreased biofilm detachment, was also observed to be impaired in virulence and intestinal colonization in an intragastric mouse model (38). In the human pathogen group A *Streptococcus*, deletion of the transcriptional regulator Srv, which is involved in regulating the SpeB extracellular cysteine protease, leads to constitutive production of SpeB (39, 40). This regulatory control of SpeB may be a mechanism for biofilm dispersal, where high levels of SpeB were correlated with increase dispersal. Indeed, *srv* mutant strains were observed to form larger lesions than wild-type strains in a murine subcutaneous infection model (39, 40). In enteropathogenic *Escherichia coli*, deletion of BfpF, which is required for the production of type IV bundle-forming pili that are necessary for biofilm dispersal, reduced virulence by about 200-fold relative to that of the wild type in a model measuring postinoculation dose-dependent diarrheal response in human volunteers (41). There is also some evidence in support of this hypothesis linking dispersal and disease progression in fungal biofilms. For example, genetic evidence in *C. albicans* suggests that deletion of Nrg1, a known dispersal regulator (20), completely attenuates virulence in a murine model of disseminated candidiasis (42). However, deletion of Nrg1 has profound effects on the morphology of planktonic cells, so it is not possible to ascribe its effects solely to biofilm dispersal. Finally, it was shown that cells dispersed from wild-type biofilms have greater virulence than standard wild-type planktonic cells in a murine disseminated infection model (15).

TABLE 1 *C. albicans* strains used in this study

Strain	Genotype	Source or reference
CJN2770	*ura3*Δ::λ*imm434*::*URA3-IRO1*/*ura3*Δ::λ*imm434 arg4*::*hisG*/*arg4*::*hisG his1*::*hisG*/*his1*::*hisG leu2*::*hisG*::*CdARG4*/*leu2*::*hisG set3*Δ::*CmLEU2*/*set3*Δ::*CdHIS1*	This study
CJN2775	*ura3*Δ::λ*imm434*::*URA3-IRO1*/*ura3*Δ::λ*imm434 arg4*::*hisG*/*arg4*::*hisG his1*::*hisG*/*his1*::*hisG leu2*::*hisG*::*CdARG4*/*leu2*::*hisG snt1*Δ::*CmLEU2*/*snt1*Δ::*CdHIS1*	This study
DHCA402	*ura3*Δ::λ*imm434*::*URA3-IRO1*/*ura3*Δ::λ*imm434 arg4*::*hisG*/*arg4*::*hisG his1*::*hisG*/*his1*::*hisG leu2*::*hisG*/*leu2*::*hisG set3*Δ::*CmLEU2*/*set3*Δ::*CdHIS1*	24
DHCA405	*ura3*Δ::λ*imm434*::*URA3-IRO1*/*ura3*Δ::λ*imm434 arg4*::*hisG*/*arg4*::*hisG his1*::*hisG*/*his1*::*hisG leu2*::*hisG*/*leu2*::*hisG set3*Δ::*CmLEU2*/*set3*Δ::*SET3-FRT*	24
DHCA406	*ura3*Δ::λ*imm434*::*URA3-IRO1*/*ura3*Δ::λ*imm434 arg4*::*hisG*/*arg4*::*hisG his1*::*hisG*/*his1*::*hisG leu2*::*hisG*/*leu2*::*hisG hos2*Δ::*CmLEU2*/*hos2*Δ::*CdHIS1*	24
DHCA420	*ura3*Δ::λ*imm434*::*URA3-IRO1*/*ura3*Δ::λ*imm434 arg4*::*hisG*/*arg4*::*hisG his1*::*hisG*/*his1*::*hisG leu2*::*hisG*/*leu2*::*hisG hos2*Δ::*CmLEU2*/*hos2*Δ::*HOS2-SAT1*	24
DHCA454	*ura3*Δ::λ*imm434*::*URA3-IRO1*/*ura3*Δ::λ*imm434 arg4*::*hisG*/*arg4*::*hisG his1*::*hisG*/*his1*::*hisG leu2*::*hisG*/*leu2*::*hisG sif2*Δ::*CmLEU2*/*sif2*Δ::*CdHIS1*	24
SN250	*ura3*Δ::λ*imm434*::*URA3-IRO1*/*ura3*Δ::λ*imm434 arg4*::*hisG*/*arg4*::*hisG his1*::*hisG*/*his1*::*hisG leu2*::*hisG*::*CdHIS1*/*leu2*::*hisG*::*CmLEU2*	29
SN855	*ura3*Δ::λ*imm434*::*URA3-IRO1*/*ura3*Δ::λ*imm434 arg4*::*hisG*/*arg4*::*hisG his1*::*hisG*/*his1*::*hisG leu2*::*hisG*/*leu2*::*hisG snt1*Δ::*CmLEU2*/*snt1*Δ::*CdHIS1*	29
SN425	*ura3*Δ::λ*imm434*::*URA3-IRO1*/*ura3*Δ::λ*imm434 arg4*::*hisG*::*CdARG4*/*arg4*::*hisG his1*::*hisG*/*his1*::*hisG leu2*::*hisG*::*CdHIS1*/*leu2*::*hisG*::*CmLEU2*	29
TF125	*ura3*Δ::λ*imm434*::*URA3-IRO1*/*ura3*Δ::λ*imm434 arg4*::*hisG*/*arg4*::*hisG his1*::*hisG*/*his1*::*hisG leu2*::*hisG*/*leu2*::*hisG nrg1*Δ::*CmLEU2*/*nrg1*Δ::*CdHIS1*	28

Our results are consistent with a correlation between biofilm dispersal and virulence. Despite the facts that the Set3 complex mutants are hyperfilamentous and form highly drug-resistant biofilms (features often associated with virulence), Set3 complex mutants are almost completely avirulent in a murine disseminated infection model (24). We postulate that, as in bacterial biofilms, decreased dispersal of cells from *C. albicans* biofilms is likely to be correlated with impaired virulence since the infecting cells would be unable to disseminate to other regions of the host. We note, however, that we cannot rule out the possibility that the loss of members of the Set3 complex may alter the expression of other, unknown, genes with effects on virulence. In this regard, it is worth noting the gene ontology enrichment categories of the RNA-seq data available for the *set3*Δ/Δ mutant compared to the wild type under hypha-inducing conditions (23). Of the 33 genes downregulated at least 2-fold in the *set3*Δ/Δ mutant, 9 have unknown biological functions, 9 are involved in drug response, and 3 play roles in septin organization and cell cycle progression, based on CGD Gene Ontology Slim Mapper (*Candida* GO-Slim Process), i.e., *GIN4*, *CCN1*, and *MCD1* (43–45) (see Table S1 in the supplemental material [DOWN set3 deletion hypha]). In addition, the gene ontology enrichment categories of these RNA-seq data also indicate that of the 116 genes upregulated at least 2-fold in the *set3*Δ/Δ mutant, 69 have unknown biological functions, 15 are involved in drug response, and 9 are implicated in septin organization and cell cycle progression on the basis of CGD Gene Ontology Slim Mapper (*Candida* GO-Slim Process), i.e., *SEP7*, *CEK1*, *DDC1*, *HAC1*, *SGO1*, *ORF19.1363*, *ORF19.2713*, *ORF19.2922*, and *ORF19.7450* (46–48) (see Table S1 in the supplemental material [UP set3 deletion hypha]). Finally, a manual inspection of the RNA-seq data indicated that there are several putative adhesins that are upregulated in the *set3*Δ/Δ mutant under both yeast- and hypha-inducing conditions, including *FLO9*, *PGA17*, *PGA22*, *PGA23*, *PGA31*, *PGA42*, *PGA45*, and *PGA58* (see Table S1 in the supplemental material [UP set3 deletion yeast and UP set3 deletion hypha]), which could contribute to the increased cohesiveness of Set3 complex mutant biofilms. Thus, the transcriptional profiling data are consistent with the roles of the Set3 complex in positively and negatively mediating drug responses, cell separation, cell cycle progression, and cell cohesiveness.

Our results may provide important information for new strategies to target biofilm dispersal as a potential antifungal intervention. In particular, our results suggest that histone deacetylase-inhibitory drugs may be useful for inhibition of biofilm dispersal and consequently prevention of the spread of a biofilm infection to new niches within the body. If these histone deacetylase-inhibitory drugs were used in combination with known antifungals with effectiveness against planktonic cells, it might be possible to control the spread of biofilm-based infections in the host. In fact, trichostatin A, a known histone deacetylase inhibitor, has been shown to induce filamentation at physiological temperatures and reduce other specific virulence attributes of *C. albicans* (24, 49). In addition, deletion of only the Set3 and Hos2 core subunits of the Set3 complex phenocopied trichostatin A treatment (24), suggesting that trichostatin A inhibition of Set3 and Hos2 is directly responsible for the effects on filamentation and possibly virulence. It was also reported that homologs of Set3 and Hos2 in *Cryptococcus neoformans* are important for the infectivity of this human fungal pathogen (50), consistent with previous findings for a role of the Set3 complex in virulence in *C. albicans* and with our findings here showing that the Set3 complex is important for dispersal.

MATERIALS AND METHODS

Strains. All of the *C. albicans* strains used in this study are in isogenic backgrounds and are listed in Table 1. DHCA406 (*hos2*Δ/Δ), DHCA454 (*sif2*Δ/Δ), SN855 (*snt1*Δ/Δ), DHCA402 (*set3*Δ/Δ), TF125 (*nrg1*Δ/Δ), and SN250 (the wild type) are in Arg^- isogenic backgrounds. Strains SN855 and DHCA402 were made Arg^+ by transformation with PmeI-digested pSN105 (29) to yield strains CJN2775 and CJN2770, respectively. The

isogenic Arg^+ wild-type strain is SN425 (29). Only prototrophic strains were tested in the *in vivo* rat catheter model. Gene complementation strains DHCA405 (*SET3* add-back strain) and DHCA420 (*HOS2* add-back strain) were previously constructed (24). In these add-back strains, all of the *in vitro* phenotypes of the mutants that we assessed in this study are reversed (data not shown). We did not test the add-back strains in the *in vivo* assays in order to minimize the number of animals used.

Media. Overnight cultures of *C. albicans* strains were grown at 30°C in YPD medium (2% Bacto Peptone, 2% dextrose, 1% yeast extract). Biofilms were grown in Spider medium (51) at 37°C, except for the drug biofilm disruption assay and the MIC assay, where biofilms were grown in RPMI 1640 medium with L-glutamine and 0.165 M morpholinepropanesulfonic acid (MOPS) and without sodium bicarbonate (Lonza 04-525F).

Six-well biofilm perturbation assay, dry-weight measurements, and crystal violet staining. Overnight cultures of *C. albicans* strains were grown in YPD medium at 30°C. By using OD_{600} measurements of each strain, a starting OD_{600} of 0.5 in 4 ml of Spider medium was calculated. Biofilms were set up to grow in six-well polystyrene, non-tissue-culture-treated plates in 4 ml of medium with five repeats and a sixth blank well control. Each well was seeded with the appropriate amount of overnight culture to achieve a starting OD_{600} of 0.5 in 4 ml of Spider medium and grown in an ELMI digital thermostatic shaker at 200 rpm at 37°C for 90 min to allow the adherence initiation step of biofilm growth. After the 90-min adherence step, medium from each well was aspirated, 4 ml of phosphate-buffered saline (PBS) was added to wash off any nonadhering cells, and the PBS was aspirated. Lastly, 4 ml of fresh Spider medium was added to each well and biofilms were grown for 24 h in an ELMI shaker as described above. To highlight the distinctive "rubbery" phenotype of the Set3 complex mutants, a perturbation assay was developed in which a plastic pipette was used to agitate the biofilm and lift the intact biofilm above the well. Unlike the Set3 complex mutant strains, agitation of the wild-type strain biofilm in this manner did not result in an intact biofilm. For dry-mass measurements, five replicate wells containing biofilms were used. The medium was removed, 2 ml of PBS was added to each well, the biofilms were disrupted by pipetting up and down, and the contents of each well were vacuum filtered over a preweighed 0.8-μm nitrocellulose filter (Millipore AAWG02500). A control well with no cells added was also vacuum filtered. The biofilm-containing filters were dried overnight and weighed the following day. The average total biomass of each strain was calculated from five independent samples after subtracting the mass of the filter with no cells added. Statistical significance (*P* values) was calculated with Student's one-tailed paired *t* test. As a complementary assay, biofilm formation was also quantified by a crystal violet assay as previously described (52). OD_{595} was read with a Tecan Infinite M1000 PRO microplate reader. The average total OD_{595} of each strain was calculated from five independent samples after subtracting the OD_{595} of a control well with no biofilm present. Statistical significance (*P* values) was calculated with Student's one-tailed paired *t* test.

***In vitro* biofilm growth for confocal microscopy.** Biofilms were grown on square (1.5 by 1.5 cm) silicone substrates (Cardiovascular Instruments Corp. PR72034-060N) as previously described (14). Strains were grown overnight in YPD medium at 30°C and diluted to a starting OD_{600} of 0.5 in 2 ml of Spider medium. Twelve-well polystyrene plates (BD Falcon) containing the silicone squares were treated overnight with 2 ml of bovine serum, washed with PBS the next morning, and inoculated with each strain. The plates were incubated at 37°C for 90 min in an ELMI digital thermostatic shaker at 200 rpm to allow cells to adhere. Plates were washed with 2 ml of PBS, 2 ml of fresh Spider medium was added to each well, and the plates were incubated at 37°C for 24 or 48 h at 200 rpm to allow biofilm formation. CSLM was used to visualize the biofilms grown on the silicone squares as previously described (16). Briefly, biofilms were stained with 50 μg/ml of concanavalin A Alexa Fluor 594 conjugate (conA-594; Molecular Probes C-11253) in the dark for 1 h with agitation at 200 rpm at 37°C. CSLM was performed at the Nikon Imaging Center (NIC) at the University of California, San Francisco (UCSF) with a Nikon Eclipse C1si upright spectral imaging confocal microscope with a 40×/0.80 W Nikon objective. For conA-594 visualization, a 561-nm laser line was used. Images were acquired by Nikon EZ-C1 version 3.80 software and assembled into top views and maximum-intensity Z-stack projections by Nikon NIS Elements version 3.00 software.

***In vivo* rat catheter biofilm model.** A well-established rat central venous catheter infection model (32) was used for *in vivo* biofilm modeling to mimic human catheter infections as described previously (32). These *in vivo* experiments were approved by the University of Wisconsin—Madison IACUC. For this animal model, specific-pathogen-free female Sprague-Dawley rats weighing 400 g (Harlan Sprague-Dawley) were used. Briefly, a heparinized (100 U/ml) polyethylene catheter with a 0.76-mm inner diameter and a 1.52-mm outer diameter was inserted into the external jugular vein and advanced to a site above the right atrium. The catheter was secured to the vein with the proximal end tunneled subcutaneously to the midscapular space and externalized through the skin. The catheters were inserted 24 h prior to infection to permit a conditioning period for deposition of host protein on the catheter surface. Infection was achieved by intraluminal instillation of 500 μl *C. albicans* cells (10^6 cells/ml). After a 4-h dwelling period, the catheter volume was withdrawn and the catheter was flushed with heparinized 0.15 M NaCl. Catheters were removed after 24 h of *C. albicans* infection to assay biofilm development on the intraluminal surface by SEM. Catheter segments were washed with 0.1 M phosphate buffer (pH 7.2), fixed in 1% glutaraldehyde–4% formaldehyde, washed again with phosphate buffer for 5 min, and placed in 1% osmium tetroxide for 30 min. The samples were dehydrated by a series of 10-min ethanol washes (30, 50, 70, 85, 95, and 100%), followed by critical-point drying. Specimens were mounted on aluminum stubs, sputter coated with gold, and imaged with a Hitachi S-5700 or a JEOL JSM-6100 scanning electron microscope in the high-vacuum mode at 10 kV. Images were assembled with Adobe Photoshop version 7.0.1 software.

Biofilm dispersal assays. Two biofilm dispersal assays were developed, a standard-dispersal assay and a sustained-dispersal assay. For the standard biofilm dispersal assay, biofilms were prepared as described for our six-well biofilm assay and cell dispersal was assessed after 24 h by carefully removing all 4 ml of medium from each well (without disturbing the biofilm adhering to the bottom of the well), taking an OD_{600} reading of the medium, and adding 4 ml of fresh Spider medium to the well, and then biofilm formation was allowed to proceed. Two additional OD_{600} readings were taken at 48 and 60 h following this procedure. Five replicate wells were used for each strain. For the sustained biofilm dispersal assay, biofilms were prepared as described for our six-well biofilm assay and cell dispersal was assessed after 24, 48, and 60 h by carefully removing all 4 ml of medium from each well (without disturbing the biofilm adhering to the bottom of the well) and taking an OD_{600} reading of the medium. Once the OD_{600} value was obtained, the biofilm was disposed of; thus, the biofilms grown for longer times were grown in their original medium without the addition of fresh medium. Five replicate wells were used for each time point for each strain. As a planktonic growth control for later time points in the sustained biofilm dispersal assay, biofilm samples removed from the medium were grown planktonically in the same biofilm spent medium for the same times as in the sustained biofilm dispersal assay and OD_{600} readings were taken. No planktonic growth was observed in the biofilm spent medium over time, indicating that the sustained biofilm dispersal assay is measuring cells dispersed from the biofilm rather than the planktonic growth of initially dispersed cells. Quantitative CFU counts of dispersed cells in the biofilm spent medium from the wild type and the Set3 complex mutants showed similar levels of cell viability in the mutant and wild-type strains.

MIC assay. MIC assays were set up to test the effects of 1,10-phenanthroline, 4-nitroquinoline *N*-oxide, caspofungin acetate, and amphotericin B on the strains. Overnight cultures were grown in YPD medium at a starting cell density of ~10^3 per well containing 200 μl of medium as previously described (33). 1,10-Phenanthroline was tested at 160, 80, 40, 20, 10, 5, 2.5, 1.25, 0.625, 0.313, 0.156, and 0 μg/ml.

4-Nitroquinoline *N*-oxide was tested at 2, 1, 0.5, 0.25, 0.125, 0.063, 0.031, 0.016, 0.008, 0.004, 0.002, and 0 μg/ml. Caspofungin acetate was tested at 500, 250, 125, 62.5, 31.25, 15.625, 3.906, 1.953, 0.977, 0.488, 0.05, 0.003, and 0 μg/ml. Amphotericin B was tested at 5, 2.5, 1.25, 0.625, 0.313, 0.156, 0.078, 0.039, 0.02, 0.01, 0.005, and 0 μg/ml. Wells were inoculated with cells after the drugs were added, and the plates were incubated statically at 30°C for 48 h. MIC assays were performed in triplicate. After incubation, the cells were resuspended by pipetting up and down and OD_{600} was read with a Tecan Infinite M1000 PRO microplate reader.

Ninety-six-well drug biofilm disruption assay. Twenty-four-hour biofilms were grown in the wells of a 96-well plate (BD Falcon) as follows. Overnight cultures were diluted to an OD_{600} of 0.5 in 0.2 ml of RPMI 1640 medium (Lonza 04-525F), and all of the wells except those in rows A and H and columns 1 and 12 were seeded with cells at that density. Medium was added to row H columns 2 to 6 as a blank control. Sterile water was added to the rest of the empty outer wells in order to control for edge effect evaporation. The plate was incubated at 37°C for 90 min at 350 rpm in an ELMI shaker to allow the initiation biofilm formation. After 90 min, the medium was aspirated and the wells were washed with 0.2 ml of PBS. Fresh medium was added to each well, and the plate was incubated for 24 h. After 24 h, the medium was aspirated and fresh medium containing a final concentration of 160 μg/ml of 1,10-phenanthroline, 2 μg/ml of 4-nitroquinoline *N*-oxide, 100 μg/ml of caspofungin acetate, or 50 μg/ml of amphotericin B was added to five replicate wells. The plates were incubated for another 24 h with the indicated drugs, medium was aspirated, and the OD_{600} values of the remaining cells adhering to the plate were read with a Tecan Infinite M1000 PRO microplate reader. Statistical significance (*P* values) was calculated with Student's one-tailed paired *t* test.

XTT biofilm cell viability assays. XTT reduction assays were performed as described previously (53), with the following modifications. Biofilms were grown as described above for the 96-well drug biofilm disruption assay. Medium was removed, and a 100-μl solution of 90% XTT (Sigma X4626; 0.5 mg/ml in PBS, filtered) plus 10% phenazine methosulfate (Sigma P9625; 0.32 mg/ml in water) was added to each well and incubated for 30 min at 37°C. The OD_{495} was read immediately on a Tecan Infinite M1000 PRO microplate reader to determine the viable biofilm cell burden. Five replicate wells were used for each strain. Statistical significance (*P* values) was calculated with Student's one-tailed paired *t* test.

Quantitative CFU biofilm cell viability assay. The viable biofilm cell burden was determined after drug treatment by physical disruption of the biofilm remaining at the bottom of the well by vortexing, followed by sonication in a water bath for 20 min as described previously (54). Disrupted biofilms were serially diluted, dilutions were plated, and viable CFU were counted. Five replicate wells were used for each strain. Statistical significance (*P* values) was calculated with Student's one-tailed paired *t* test.

Real-time qPCR. Expression levels of the multidrug efflux pump genes (*CDR1*, *CDR2*, *CDR3*, and *MDR1*) were measured in the background of each of the core Set3 complex mutants by real-time quantitative PCR (qPCR) with the following primer pairs: CJNO1456 (5′ CTAAGATGTCGTCGCAAGATGAATC 3′) and CJNO1457 (5′ GGCATTGAAATTTTCTGAATCGG 3′) for *CDR1*, CJNO1458 (5′ CAAACACGTCTTTGTCGCAACAG 3′) and CJNO1459 (5′ GGCATTGAAATTTTCGGAATCTG 3′) for *CDR2*, CJNO1460 (5′ GTTGGGTGTTATTGGTGCTGCT 3′) and CJNO1461 (5′ TCCATTAAACAAGGAACACAACACAG 3′) for *CDR3*, and CJNO1462 (5′ CAGATTTTTGAGAGATAGTTTTGTTGG 3′) and CJNO1463 (5′ CCCAAGTGACAACTATTTTATCTCCATC 3′) for *MDR1*. Expression levels were assessed under biofilm conditions. Normalized gene expression values were calculated by the $\Delta\Delta C_T$ method by using *TAF145* as a reference gene. Results are the means of three determinations.

FDA assay. For the biofilm FDA assay, strains were grown overnight in YPD while shaking at 30°C. Biofilms were grown in the standard 96-well biofilm assay (described above) in an optical-bottom plate (Nunc 165305). The biofilm in each well was washed with 200 μl of water and then 200 μl of FDA buffer (50 mM HEPES [pH 7.0], 5 mM 2-deoxy-D-glucose). A 200-μl volume of FDA buffer with or without FDA (Molecular Probes F1303; dissolved in dimethyl sulfoxide) was added to each well. For the planktonic FDA assay, cells were diluted to an OD_{600} of 0.1 in YPD and grown for 5 h while shaking at 30°C. Cells at an OD_{600} of 1of were washed once with sterile water and once with FDA buffer. A 1.3-ml volume of cell suspension was mixed with 3 μl of 5 mM FDA. A 200-μl volume of cell mixture with or without FDA was added to an optical-bottom 96-well plate.

For both planktonic and biofilm FDA assays, fluorescence was measured on a Tecan M200 plate reader with an excitation wavelength of 485 nm and an emission wavelength of 535 nm at 30°C with shaking every 5 min for 30 reads or until saturation was reached. At least 10 technical replicates and at least 2 biological replicates were measured for each strain and condition.

***In vitro* biofilm matrix β-1,3-glucan level measurements.** Biofilm matrix β-1,3-glucan level measurements were performed as described previously (55), with the following modifications. Biofilms were grown for 24 h on bovine serum-coated six-well polystyrene plates in RPMI medium. Biofilm matrix was harvested by removing all of the spent medium and then adding 700 μl of sterile water, scraping the cells with a cell scraper, and collecting them in a microcentrifuge tube. This step was repeated with a fresh 700 μl of sterile water, and collections were combined. Cells were sonicated in a Diagenode Bioruptor water bath sonicator at high power (settings: 1 min on, 30 s off) for 10 min. Cells were centrifuged at 4,500 × *g* and 4°C for 20 min, and the supernatant was collected, frozen in liquid nitrogen, and stored at −80°C. To measure soluble β-1,3-glucan levels in the matrix, samples were diluted 1/1,000 and 1/5,000 and 50 μl of diluted sample was measured with a Glucatell (1,3)-β-D-glucan detection reagent kit (Cape Cod Incorporated GD12002) by following the manufacturer's protocol for an endpoint assay. Measurements were performed in triplicate. Glucatell kit readouts were measured on a Tecan Infinite PRO M200 microplate reader at 550 nm.

SUPPLEMENTAL MATERIAL

Supplemental material for this article may be found at http://mbio.asm.org/lookup/suppl/doi:10.1128/mBio.01201-14/-/DCSupplemental.

Figure S1, PDF file, 0.7 MB.
Figure S2, PDF file, 0.2 MB.
Figure S3, PDF file, 0.2 MB.
Figure S4, PDF file, 0.2 MB.
Figure S5, PDF file, 0.1 MB.
Figure S6, PDF file, 0.2 MB.
Table S1, XLSX file, 0.1 MB.

ACKNOWLEDGMENTS

The research reported in this publication was supported by National Institutes of Health (NIH) grants K99AI100896 (C.J.N.), R01AI073289 (D.R.A.), and R01AI083311 (A.D.J.). K.K. was supported by grant FWF-P25333-B22-Chromatin from the Austrian Science Fund and in part by a grant from the Christian Doppler Society. The content is solely our responsibility and does not represent the official views of the funding agencies.

We thank Richard Bennett and Aaron Hernday for comments on the manuscript and Sheena Singh-Babak for advice on the MIC and drug biofilm disruption assays. We are grateful for the availability of the NIC at UCSF, where the CSLM images were acquired.

REFERENCES

1. **Donlan RM, Costerton JW.** 2002. Biofilms: survival mechanisms of clinically relevant microorganisms. Clin. Microbiol. Rev. **15:**167–193. http://dx.doi.org/10.1128/CMR.15.2.167-193.2002.
2. **Kojic EM, Darouiche RO.** 2004. *Candida* infections of medical devices. Clin. Microbiol. Rev. **17:**255–267. http://dx.doi.org/10.1128/CMR.17.2.255-267.2004.
3. **Donlan RM.** 2001. Biofilm formation: a clinically relevant microbiologi-

cal process. Clin. Infect. Dis. **33:**1387–1392. http://dx.doi.org/10.1086/322972.
4. **Douglas LJ.** 2002. Medical importance of biofilms in Candida infections. Rev. Iberoam. Micol. **19:**139–143. http://www.reviberoammicol.com/2002-19/139143.pdf.
5. **Douglas LJ.** 2003. Candida biofilms and their role in infection. Trends Microbiol. **11:**30–36. http://dx.doi.org/10.1016/S0966-842X(02)00002-1.
6. **Wenzel RP.** 1995. Nosocomial candidemia: risk factors and attributable mortality. Clin. Infect. Dis. **20:**1531–1534. http://dx.doi.org/10.1093/clinids/20.6.1531.
7. **Akins RA.** 2005. An update on antifungal targets and mechanisms of resistance in Candida albicans. Med. Mycol. **43:**285–318. http://dx.doi.org/10.1080/13693780500138971.
8. **Mathé L, Van Dijck P.** 2013. Recent insights into *Candida albicans* biofilm resistance mechanisms. Curr. Genet. **59:**251–264. http://dx.doi.org/10.1007/s00294-013-0400-3.
9. **Ramage G, Rajendran R, Sherry L, Williams C.** 2012. Fungal biofilm resistance. Int. J. Microbiol. 2012:528521. http://dx.doi.org/10.1155/2012/528521.
10. **Taff HT, Mitchell KF, Edward JA, Andes DR.** 2013. Mechanisms of Candida biofilm drug resistance. Future Microbiol. **8:**1325–1337. http://dx.doi.org/10.2217/fmb.13.101.
11. **Hawser SP, Douglas LJ.** 1994. Biofilm formation by *Candida* species on the surface of catheter materials in vitro. Infect. Immun. **62:**915–921.
12. **Baillie GS, Douglas LJ.** 1999. Role of dimorphism in the development of *Candida albicans* biofilms. J. Med. Microbiol. **48:**671–679. http://dx.doi.org/10.1099/00222615-48-7-671.
13. **Chandra J, Kuhn DM, Mukherjee PK, Hoyer LL, McCormick T, Ghannoum MA.** 2001. Biofilm formation by the fungal pathogen *Candida albicans*: development, architecture, and drug resistance. J. Bacteriol. **183:**5385–5394. http://dx.doi.org/10.1128/JB.183.18.5385-5394.2001.
14. **Nobile CJ, Mitchell AP.** 2005. Regulation of cell-surface genes and biofilm formation by the *C. albicans* transcription factor Bcr1p. Curr. Biol. **15:**1150–1155. http://dx.doi.org/10.1016/j.cub.2005.05.047.
15. **Uppuluri P, Chaturvedi AK, Srinivasan A, Banerjee M, Ramasubramaniam AK, Köhler JR, Kadosh D, Lopez-Ribot JL.** 2010. Dispersion as an important step in the *Candida albicans* biofilm developmental cycle. PLoS Pathog. **6:**e1000828. http://dx.doi.org/10.1371/journal.ppat.1000828.
16. **Nobile CJ, Fox EP, Nett JE, Sorrells TR, Mitrovich QM, Hernday AD, Tuch BB, Andes DR, Johnson AD.** 2012. A recently evolved transcriptional network controls biofilm development in *Candida albicans*. Cell **148:**126–138. http://dx.doi.org/10.1016/j.cell.2011.10.048.
17. **Fox EP, Nobile CJ.** 2012. A sticky situation: untangling the transcriptional network controlling biofilm development in *Candida albicans*. Transcription **3:**315–322. http://dx.doi.org/10.4161/trns.22281.
18. **Chen C, Pande K, French SD, Tuch BB, Noble SM.** 2011. An iron homeostasis regulatory circuit with reciprocal roles in *Candida albicans* commensalism and pathogenesis. Cell Host Microbe **10:**118–135. http://dx.doi.org/10.1016/j.chom.2011.07.005.
19. **Finkel JS, Xu W, Huang D, Hill EM, Desai JV, Woolford CA, Nett JE, Taff H, Norice CT, Andes DR, Lanni F, Mitchell AP.** 2012. Portrait of *Candida albicans* adherence regulators. PLoS Pathog. **8:**e1002525. http://dx.doi.org/10.1371/journal.ppat.1002525.
20. **Uppuluri P, Pierce CG, Thomas DP, Bubeck SS, Saville SP, Lopez-Ribot JL.** 2010. The transcriptional regulator Nrg1p controls *Candida albicans* biofilm formation and dispersion. Eukaryot. Cell **9:**1531–1537. http://dx.doi.org/10.1128/EC.00111-10.
21. **Lu Y, Su C, Liu H.** 2012. A GATA transcription factor recruits Hda1 in response to reduced Tor1 signaling to establish a hyphal chromatin state in *Candida albicans*. PLoS Pathog. **8:**e1002663. http://dx.doi.org/10.1371/journal.ppat.1002663.
22. **Lu Y, Su C, Mao X, Raniga PP, Liu H, Chen J.** 2008. Efg1-mediated recruitment of NuA4 to promoters is required for hypha-specific Swi/Snf binding and activation in *Candida albicans*. Mol. Biol. Cell **19:**4260–4272. http://dx.doi.org/10.1091/mbc.E08-02-0173.
23. **Hnisz D, Bardet AF, Nobile CJ, Petryshyn A, Glaser W, Schöck U, Stark A, Kuchler K.** 2012. A histone deacetylase adjusts transcription kinetics at coding sequences during *Candida albicans* morphogenesis. PLoS Genet. **8:**e1003118. http://dx.doi.org/10.1371/journal.pgen.1003118.
24. **Hnisz D, Majer O, Frohner IE, Komnenovic V, Kuchler K.** 2010. The Set3/Hos2 histone deacetylase complex attenuates cAMP/PKA signaling to regulate morphogenesis and virulence of *Candida albicans*. PLoS Pathog. **6:**e1000889. http://dx.doi.org/10.1371/journal.ppat.1000889.
25. **Lopes da Rosa J, Boyartchuk VL, Zhu LJ, Kaufman PD.** 2010. Histone acetyltransferase Rtt109 is required for *Candida albicans* pathogenesis. Proc. Natl. Acad. Sci. U. S. A. **107:**1594–1599. http://dx.doi.org/10.1073/pnas.0912427107.
26. **Raman SB, Nguyen MH, Zhang Z, Cheng S, Jia HY, Weisner N, Iczkowski K, Clancy CJ.** 2006. *Candida albicans* SET1 encodes a histone 3 lysine 4 methyltransferase that contributes to the pathogenesis of invasive candidiasis. Mol. Microbiol. **60:**697–709. http://dx.doi.org/10.1111/j.1365-2958.2006.05121.x.
27. **Pijnappel WW, Schaft D, Roguev A, Shevchenko A, Tekotte H, Wilm M, Rigaut G, Séraphin B, Aasland R, Stewart AF.** 2001. The *S. cerevisiae* SET3 complex includes two histone deacetylases, Hos2 and Hst1, and is a meiotic-specific repressor of the sporulation gene program. Genes Dev. **15:**2991–3004. http://dx.doi.org/10.1101/gad.207401.
28. **Homann OR, Dea J, Noble SM, Johnson AD.** 2009. A phenotypic profile of the *Candida albicans* regulatory network. PLoS Genet. **5:**e1000783. http://dx.doi.org/10.1371/journal.pgen.1000783.
29. **Noble SM, French S, Kohn LA, Chen V, Johnson AD.** 2010. Systematic screens of a *Candida albicans* homozygous deletion library decouple morphogenetic switching and pathogenicity. Nat. Genet. **42:**590–598. http://dx.doi.org/10.1038/ng.605.
30. **Nobile CJ, Andes DR, Nett JE, Smith FJ, Yue F, Phan QT, Edwards JE, Filler SG, Mitchell AP.** 2006. Critical role of Bcr1-dependent adhesins in *C. albicans* biofilm formation in vitro and in vivo. PLoS Pathog. **2:**e63. http://dx.doi.org/10.1371/journal.ppat.0020063.
31. **Nett J, Andes D.** 2006. Candida albicans biofilm development, modeling a host-pathogen interaction. Curr. Opin. Microbiol. **9:**340–345. http://dx.doi.org/10.1016/j.mib.2006.06.007.
32. **Andes D, Nett J, Oschel P, Albrecht R, Marchillo K, Pitula A.** 2004. Development and characterization of an in vivo central venous catheter *Candida albicans* biofilm model. Infect. Immun. **72:**6023–6031. http://dx.doi.org/10.1128/IAI.72.10.6023-6031.2004.
33. **Singh SD, Robbins N, Zaas AK, Schell WA, Perfect JR, Cowen LE.** 2009. Hsp90 governs echinocandin resistance in the pathogenic yeast *Candida albicans* via calcineurin. PLoS Pathog. **5:**e1000532. http://dx.doi.org/10.1371/journal.ppat.1000532.
34. **Breeuwer P, Drocourt JL, Bunschoten N, Zwietering MH, Rombouts FM, Abee T.** 1995. Characterization of uptake and hydrolysis of fluorescein diacetate and carboxyfluorescein diacetate by intracellular esterases in *Saccharomyces cerevisiae*, which result in accumulation of fluorescent product. Appl. Environ. Microbiol. **61:**1614–1619.
35. **Nett J, Lincoln L, Marchillo K, Massey R, Holoyda K, Hoff B, VanHandel M, Andes D.** 2007. Putative role of beta-1,3-glucans in *Candida albicans* biofilm resistance. Antimicrob. Agents Chemother. **51:**510–520. http://dx.doi.org/10.1128/AAC.01056-06.
36. **Kaplan JB.** 2010. Biofilm dispersal: mechanisms, clinical implications, and potential therapeutic uses. J. Dent. Res. **89:**205–218. http://dx.doi.org/10.1177/0022034509359403.
37. **Karatan E, Watnick P.** 2009. Signals, regulatory networks, and materials that build and break bacterial biofilms. Microbiol. Mol. Biol. Rev. **73:**310–347. http://dx.doi.org/10.1128/MMBR.00041-08.
38. **Kim SM, Park JH, Lee HS, Kim WB, Ryu JM, Han HJ, Choi SH.** 2013. LuxR homologue SmcR is essential for *Vibrio vulnificus* pathogenesis and biofilm detachment, and its expression is induced by host cells. Infect. Immun. **81:**3721–3730. http://dx.doi.org/10.1128/IAI.00561-13.
39. **Connolly KL, Braden AK, Holder RC, Reid SD.** 2011. Srv mediated dispersal of streptococcal biofilms through SpeB is observed in CovRS$^+$ strains. PLoS One **6:**e28640. http://dx.doi.org/10.1371/journal.pone.0028640.
40. **Connolly KL, Roberts AL, Holder RC, Reid SD.** 2011. Dispersal of group A streptococcal biofilms by the cysteine protease SpeB leads to increased disease severity in a murine model. PLoS One **6:**e18984. http://dx.doi.org/10.1371/journal.pone.0018984.
41. **Bieber D, Ramer SW, Wu CY, Murray WJ, Tobe T, Fernandez R, Schoolnik GK.** 1998. Type IV pili, transient bacterial aggregates, and virulence of enteropathogenic *Escherichia coli*. Science **280:**2114–2118. http://dx.doi.org/10.1126/science.280.5372.2114.
42. **Murad AM, Leng P, Straffon M, Wishart J, Macaskill S, MacCallum D, Schnell N, Talibi D, Marechal D, Tekaia F, d'Enfert C, Gaillardin C, Odds FC, Brown AJ.** 2001. NRG1 represses yeast-hypha morphogenesis and hypha-specific gene expression in *Candida albicans*. EMBO J. **20:**4742–4752. http://dx.doi.org/10.1093/emboj/20.17.4742.
43. **Wightman R, Bates S, Amornrrattanapan P, Sudbery P.** 2004. In *Can-*

dida albicans, the Nim1 kinases Gin4 and Hsl1 negatively regulate pseudohypha formation and Gin4 also controls septin organization. J. Cell Biol. **164:**581–591. http://dx.doi.org/10.1083/jcb.200307176.

44. **Sinha I, Wang YM, Philp R, Li CR, Yap WH, Wang Y.** 2007. Cyclin-dependent kinases control septin phosphorylation in *Candida albicans* hyphal development. Dev. Cell **13:**421–432. http://dx.doi.org/10.1016/j.devcel.2007.06.011.
45. **Clarke DJ, Giménez-Abián JF.** 2000. Checkpoints controlling mitosis. Bioessays **22:**351–363. http://dx.doi.org/10.1002/(SICI)1521-1878(200004)22:4<351::AID-BIES5>3.0.CO;2-W.
46. **González-Novo A, Correa-Bordes J, Labrador L, Sánchez M, Vázquez de Aldana CR, Jiménez J.** 2008. Sep7 is essential to modify septin ring dynamics and inhibit cell separation during *Candida albicans* hyphal growth. Mol. Biol. Cell **19:**1509–1518. http://dx.doi.org/10.1091/mbc.E07-09-0876.
47. **Whiteway M, Dignard D, Thomas DY.** 1992. Dominant negative selection of heterologous genes: isolation of *Candida albicans* genes that interfere with *Saccharomyces cerevisiae* mating factor-induced cell cycle arrest. Proc. Natl. Acad. Sci. U. S. A. **89:**9410–9414. http://dx.doi.org/10.1073/pnas.89.20.9410.
48. **Côte P, Hogues H, Whiteway M.** 2009. Transcriptional analysis of the *Candida albicans* cell cycle. Mol. Biol. Cell **20:**3363–3373. http://dx.doi.org/10.1091/mbc.E09-03-0210.
49. **Simonetti G, Passariello C, Rotili D, Mai A, Garaci E, Palamara AT.** 2007. Histone deacetylase inhibitors may reduce pathogenicity and virulence in *Candida albicans*. FEMS Yeast Res. **7:**1371–1380. http://dx.doi.org/10.1111/j.1567-1364.2007.00276.x.
50. **Liu OW, Chun CD, Chow ED, Chen C, Madhani HD, Noble SM.** 2008. Systematic genetic analysis of virulence in the human fungal pathogen *Cryptococcus neoformans*. Cell **135:**174–188. http://dx.doi.org/10.1016/j.cell.2008.07.046.
51. **Liu H, Köhler J, Fink GR.** 1994. Suppression of hyphal formation in *Candida albicans* by mutation of a STE12 homolog. Science **266:**1723–1726. http://dx.doi.org/10.1126/science.7992058.
52. **Jin Y, Yip HK, Samaranayake YH, Yau JY, Samaranayake LP.** 2003. Biofilm-forming ability of *Candida albicans* is unlikely to contribute to high levels of oral yeast carriage in cases of human immunodeficiency virus infection. J. Clin. Microbiol. **41:**2961–2967. http://dx.doi.org/10.1128/JCM.41.7.2961-2967.2003.
53. **Nett JE, Cain MT, Crawford K, Andes DR.** 2011. Optimizing a *Candida* biofilm microtiter plate model for measurement of antifungal susceptibility by tetrazolium salt assay. J. Clin. Microbiol. **49:**1426–1433. http://dx.doi.org/10.1128/JCM.02273-10.
54. **Taff HT, Nett JE, Andes DR.** 2012. Comparative analysis of Candida biofilm quantitation assays. Med. Mycol. **50:**214–218. http://dx.doi.org/10.3109/13693786.2011.580016.
55. **Nobile CJ, Nett JE, Hernday AD, Homann OR, Deneault JS, Nantel A, Andes DR, Johnson AD, Mitchell AP.** 2009. Biofilm matrix regulation by *Candida albicans* Zap1. PLoS Biol. **7:**e1000133. http://dx.doi.org/10.1371/journal.pbio.1000133.